Near coincidence of metal-insulator transition and quantum critical fluctuations: Electronic ground state and magnetic order in Fe$_{1-x}$Co$_x$Si

J. Grefe [1,*], P. Herre,[1] Y. Hilgers,[1] F. Labbus,[1] N. Lüer-Epping,[1] N. Radomski,[1] M. A. C. de Melo [1,2],
F. J. Litterst [1], D. Menzel [1], and S. Süllow [1]

[1]*Institut für Physik der Kondensierten Materie, TU Braunschweig, D-38106 Braunschweig, Germany*
[2]*Departamento de Fisica, Universidade Estadual de Maringá, Maringá, PR, 87020-900, Brazil*

We present a detailed study of the electronic and magnetic ground-state properties of Fe$_{1-x}$Co$_x$Si using a combination of macroscopic and microscopic experimental techniques. From these experiments we quantitatively characterize the metal-insulator transition and magnetic/nonmagnetic quantum phase transition occurring at low-doping levels in Fe$_{1-x}$Co$_x$Si. From our study, we find a surprising closeness of the critical composition of the metal-insulator transition at $x_{MIT} = 0.014$ and the quantum phase transition at $x_{LRO} \sim 0.024 - 0.031$. This suggests that these effects are cooperative and depend on each other.

I. INTRODUCTION

The class of $B20$ materials (Fe, Co, Mn)Si has been studied for decades, representing model compounds in various contexts of modern solid-state physics. The materials crystallize in the cubic $B20$ crystal structure [1] (Fig. 1). It is also labeled the *FeSi*-structure, as early on the compound was the most prominent representative of this crystallographic lattice that lacks inversion symmetry [2]. Moreover, FeSi was the first material to attract attention with respect to its electronic and magnetic properties, with initial reports on a "semiconductive and metallic" ground state [3,4] in the presence of an unusual magnetic behavior from "correlated magnetic excitations" [5]. MnSi, instead, was characterized as a ferromagnetic metal, while CoSi was reported as semimetallic diamagnet [4].

Subsequently, these observations were substantially refined. By now, MnSi has been established as a helimagnetic metal (for a review, see Pfleiderer *et al.* [6]), where helimagnetism arises from the action of the Dzyaloshinskii-Moriya interaction [7] induced by the lack of inversion symmetry in the lattice. As result of the interplay of complex magnetic couplings and anisotropies a novel magnetic state, the *skyrmion lattice*, emerges in certain parameter ranges of the magnetic phase diagram [8]. For CoSi, recently the description was complemented by the realization that for a crystal structure lacking inversion symmetry in the presence of spin-orbit coupling it gives rise to new topological electronic states [9–11].

Regarding FeSi, for a long time the central scientific issue was the nature of the small-gap semiconducting ground state [12,13]. It was proposed that this may be understood as signatures of a Kondo insulating state, i.e., a semiconducting state arising as result of strong electronic correlations. Subsequent experimental tests of this concept have not produced clear-cut evidence in favor of this scenario [14,15]. Instead, it appears that single-electron band structure modeling is sufficient to account for the observed electronic ground state. More recently, topological aspects of the band structure of FeSi have attracted attention [16]. In the present context, with respect to the electronic properties we will consider the bulk material FeSi as intrinsically gapped material, i.e., an insulator in the traditional sense, which has metallic surface states [17]. If these surface states reflect the character of a 3D topological insulator will not be addressed with our study.

Another line of inquiry regarding these $B20$ compounds are alloying studies. With a full elemental solubility, alloying studies on Fe$_{1-x-y}$Co$_x$Mn$_y$Si allow to investigate both zero-temperature (quantum phase) transitions of the electronic and magnetic ground states. Special focus lies upon the phase diagram of Fe$_{1-x}$Co$_x$Si, where a multitude of studies have been carried out in the course of 50 years of research [14,15,18–59].

The general findings with respect to magnetic order are well established [18,19,22–26,29,30,34–36,38,41,43–45,51,55–59]: The series starts with the paramagnetic small gap insulator FeSi. Already alloying in the percentage range with Co closes the gap and induces the onset of long-range helimagnetic order below T_{HM}, with a maximum ordering temperature in the range of a few 10 K. Magnetic order is fully suppressed at $x = 0.8$, and with larger x the series further transforms into the topological semimetal CoSi. In the magnetically ordered regime it is possible to identify field-induced skyrmionic phases [45,47,50,52,53,55,56]. Since the parameter range of the formation of skyrmions in Fe$_{1-x}$Co$_x$Si is very different from that of MnSi, it has enriched the possibilities to quantitatively study the physics of skyrmionic spin textures.

In detail, however, the magnetic and electronic phase diagram of Fe$_{1-x}$Co$_x$Si is far from well established. To illustrate this point, in Fig. 2 we summarize the helimagnetic transition temperatures T_{HM} for samples of the series Fe$_{1-x}$Co$_x$Si reported in the literature. Here, the variations of the transition temperatures for a given composition exhibit a very large variation (even in the maximum of the T_{HM} dome by 30%), which in other scientific contexts (high-T_C materials, quantum phase transitions etc.) would be considered unacceptable.

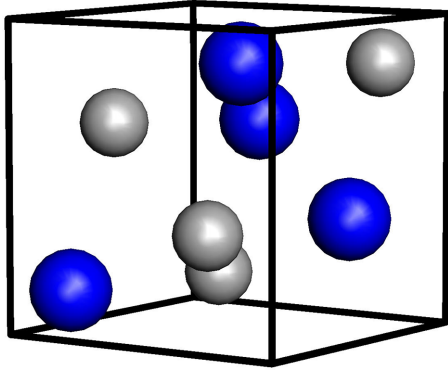*Corresponding author: j.grefe@tu-braunschweig.de

FIG. 1. Cubic *B*20 crystal structure for FeSi, with blue and grey spheres representing Fe and Si, respectively (lattice parameter $a \sim 4.48$ Å).

As pointed out by Bauer, Garst, and Pfleiderer [55], part of the problem are the different definitions and criteria chosen in literature to define the phase transition temperature T_{HM}. In Ref. [55] this was illustrated by using different criteria on their selected samples $\mathrm{Fe_{1-x}Co_xSi}$ to extract T_{HM}, leading to a large error bar in the determination of T_{HM} (up to ± 7 K). Still, Fig. 2 demonstrates that it does not fully account for the scatter of the data, and other effects need to be considered. These could be related to the use of poly- vs single-crystalline samples, differing metallurgical treatment, inaccuracies in determining the correct stoichiometry (FeSi has a homogeneity range of formation), or—given that the literature reports span a range of 50 years—simple thermometry issues etc. in certain studies. At any rate, at this point a full, thorough, and reproducible determination by well-established techniques and criteria of the phase diagram of $\mathrm{Fe_{1-x}Co_xSi}$ is lacking. In particular, scientific topics with regard to the relationship of the metal-insulator transition (MIT) occurring in $\mathrm{Fe_{1-x}Co_xSi}$ at [18,34] $x \sim 0.005 - 0.018$ and the quantum phase transition (QPT) into a long-range magnetically ordered state at larger Co
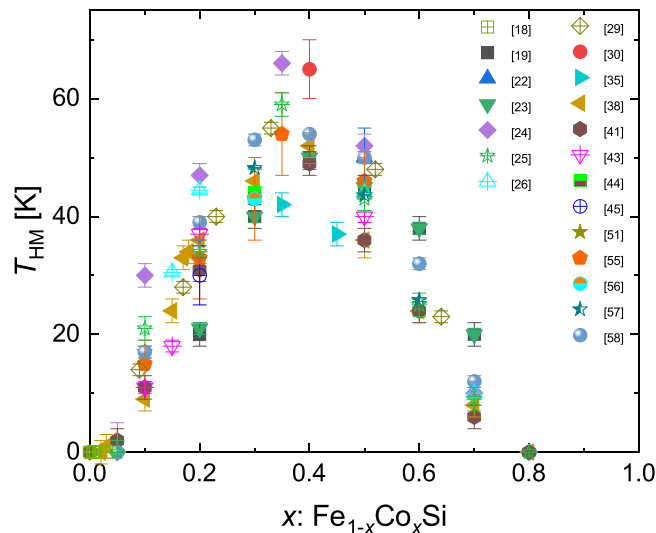

FIG. 2. Helimagnetic ordering temperatures T_{HM} of $\mathrm{Fe_{1-x}Co_xSi}$, as taken from the literature (Refs. are listed in the legend).
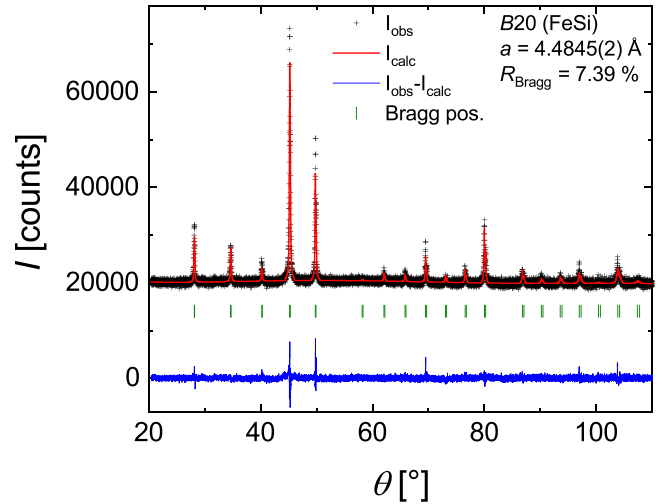

FIG. 3. Powder x-ray diffraction pattern as function of angle for FeSi. Rietveld refinement carried out using the *B*20 structure with lattice parameter indicated.

concentrations are simply not accessible with the published data.

In this situation, we have set out to reinvestigate the phase diagram of $\mathrm{Fe_{1-x}Co_xSi}$. Our particular focus lies on the small-x range, i.e., $x \leqslant 0.15$, that is the range that encloses the MIT and the QPT. For our set of single-crystalline samples we perform a thorough characterization by various bulk experimental techniques accompanied by the microscopic technique Mössbauer spectroscopy. Taken together, we aim to shed light in particular on the physical phenomena occurring at small values x, that is the regime of magnetic quantum criticality and metal-insulator transition.

II. EXPERIMENTAL DETAILS

In the choice of our samples, we restrict ourselves entirely on single-crystalline specimens obtained by the Czochralski-method using a three-arc oven as described previously [14,15]. In the low-doping regime, between different samples, we choose particularly small variations of x down to 0.01, to accurately define the details of the magnetic phase diagram and electronic ground-state properties. After growth, the samples have been oriented by means of Laue x-ray diffraction and bar-shaped samples have been cut along the cubic main axis from the crystals for bulk studies, while thin (a few ten µm) single-crystalline slices have been prepared for Mössbauer spectroscopy.

For each of the crystals some material has been ground to powder and checked by powder x-ray diffraction for phase homogeneity, crystal structure, and lattice parameters. In the powder diffraction experiments no secondary phases have been detected and the crystal structure was verified as cubic *B*20 lattice. As an example, in Fig. 3 we depict the x-ray diffraction pattern for FeSi, including a Rietveld refinement of the data. Results of similar quality are observed for the other samples, including some with larger x to cover the full phase diagram. With the similarity in x-ray scattering cross sections of Fe and Co, an analysis of the actual composition

TABLE I. Lattice and positional parameters in the $B20$ structure of $Fe_{1-x}Co_xSi$, derived from room-temperature powder x-ray diffraction.

x	a (Å)	Fe/Co	Si
0	4.4845(2)	0.134(1)	0.837(2)
0.01	4.4842(2)	0.137(2)	0.842(2)
0.02	4.4867(2)	0.136(1)	0.843(2)
0.03	4.4859(1)	0.135(2)	0.848(2)
0.04	4.4846(2)	0.138(1)	0.846(2)
0.05	4.4851(3)	0.139(1)	0.837(2)
0.06	4.4830(4)	0.137(7)	0.845(10)
0.08	4.4816(10)	0.137(7)	0.843(8)
0.15	4.4809(4)	0.138(6)	0.843(8)
0.30	4.4756(1)	0.137(1)	0.841(1)
0.55	4.4664(1)	0.141(1)	0.840(1)
0.80	4.4561(1)	0.140(1)	0.836(1)
1	4.4423(5)	0.145(8)	0.844(11)

FIG. 4. (a) Comparison of the normalized resistivity $\rho/\rho_{300\,K}$ of single-crystalline FeSi measured on a bar-shaped and a thin-plate sample. (b) Susceptibility for the same two samples FeSi.

of our specimens cannot be carried out with a sufficiently high accuracy. Therefore, in the refinements we have used the nominal composition as fixed parameter.

From the x-ray analysis we obtain the evolution of the cubic lattice parameter as function of alloying, which we list in Table I. According to Vegard's law, with the lattice parameter of FeSi, $a = 4.4845$ Å, significantly larger than that of CoSi, $a = 4.4423$ Å, a (close to) linear shrinking of the lattice parameter would be expected with Co doping [60]. Broadly speaking, this is observed experimentally in the alloying dependence of the lattice parameter. The other main free structural parameters in the $B20$ structure, the x, y, z position of (Fe/Co) and Si, remain basically constant at ~0.14 (Fe/Co) and ~0.84 (Si) within experimental scatter.

To characterize the single crystals $Fe_{1-x}Co_xSi$ regarding their electronic and magnetic properties we have carried out a standardized set of experiments. We report on the resistivity, magnetization, susceptibility and Mössbauer spectra, all in the ^{4}He-temperature range, i.e., 1.6 to 300 K. For the resistivity we used a standard four-probe ac setup. Magnetization and susceptibility have been measured using a commercial SQUID system in fields up to 5 T.

Mössbauer experiments have been performed in a standard transmission geometry employing a 50 mCi ^{57}Co source in Rh matrix. The samples used as absorbers obtained from several grinding and polishing runs of single-crystalline plates have been almost circular platelets (surface perpendicular to [100]) with maximum planar dimensions of 6 mm diameter and thickness of about 50 μm. The gamma ray direction was along [100]. The Mössbauer velocity drive system was run in sinusoidal mode. The measurements were carried out in a liquid helium bath cryostat in under-pressure mode enabling experimental temperatures down to 1.7 K.

III. RESULTS

Prior to a detailed investigation of the electronic and magnetic phase diagram of $Fe_{1-x}Co_xSi$, we need to establish the relevance of the metallic surface states for the interpretation of the experimental data. To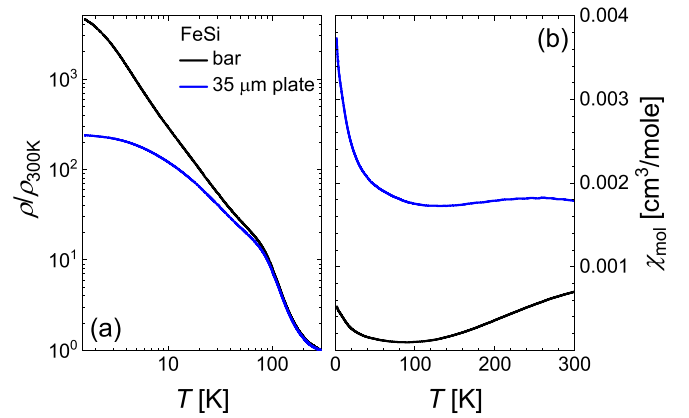 this end, we utilize the argument put forth for topological insulators that the resistivity may be modeled as superposition of surface and volume electrical conduction [61,65]. This observation implies that the relevance of surface conduction depends on the surface-to-volume ratio of a given sample [17]. We prepared two specimens of our single crystal FeSi for resistivity measurements: first, a bar-shaped sample of dimensions $5 \times 1 \times 1$ mm^3, and secondly, a sample of similar length and width, but with a thickness polished down to 35 μm, i.e., with a surface-to-volume ratio increased by a factor of about 30.

In Fig. 4(a) we compare these two samples with respect to the normalized resistivity $\rho/\rho_{300\,K}$ in a log-log-representation. From the figure it is evident that the normalized resistivity of the thin plate deviates from that of the bar-shaped sample below about 100 K. This finding is qualitatively in line with the observation of Fang et al. [17] of a metal-to-semiconductor transition in differently sized single crystals FeSi. It verifies the existence of a significant electrical surface conductivity in FeSi, which at low temperatures partially masks the insulating behavior of the bulk of the sample. As we show below, doping with Co in $Fe_{1-x}Co_xSi$ substantially increases bulk conductivity, and thus reduces the relevance of surface conductivity. Effectively, we find that we can disregard conduction from such surface states in a resistivity measurement at least for doping with Co of more than one percent.

We have also measured the magnetic susceptibility for our two samples FeSi, plotted in Fig. 4(b). It has previously been noted that even for single-crystalline FeSi there is always a low-temperature upturn of the susceptibility [5,13]. It is usually associated to magnetic (Fe) impurities, although it has been impossible to suppress or diminish this impurity contribution by different preparation techniques. As can be seen, also for our bar-shaped crystal FeSi we observe the typical behavior [5] with a broad susceptibility maximum above room temperature and the Curie tail at low temperatures. Remarkably, our thin plate sample has a substantially (an order of magnitude at low T) increased Curie-like susceptibility background. First, this observation may suggest that polishing the sample damages the surface to the effect that free Fe particles are produced, giving rise to a larger Curie tail. Secondly, and more exotically, these magnetic particles will reside on
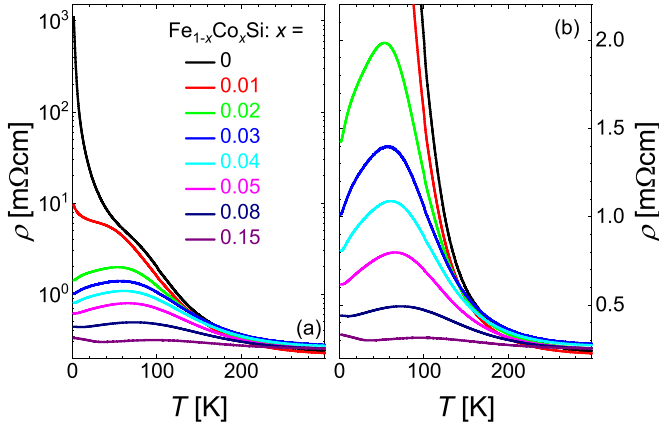
FIG. 5. Temperature-dependent zero-field resistivity $\rho(T)$ of $Fe_{1-x}Co_xSi$, $0 \leqslant x \leqslant 0.15$, (a) plotted on a logarithmic and (b) linear scale.

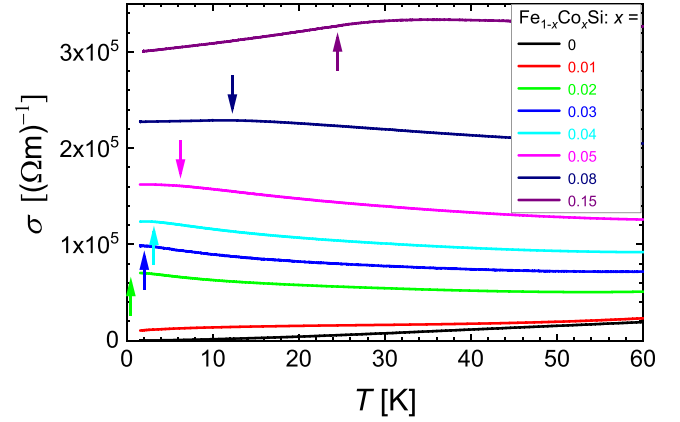FIG. 6. Temperature-dependent zero-field conductivity $\sigma(T)$ of $Fe_{1-x}Co_xSi$, $0 \leqslant x \leqslant 0.15$. Arrows denote magnetic ordering temperatures T_{HM}.

the surface of the sample, that is in the spatial range of the conducting surface states. It raises the question about the interplay of electronic and magnetic properties in particular at the surface of FeSi, and the possibility that the existence and residual coupling of magnetic moments is associated to a local metallic environment.

Having thus characterized the relevance of metallic surface states, we proceed with the zero-field resistivity of our single-crystalline bar-shaped samples $Fe_{1-x}Co_xSi$. In Fig. 5 we plot the resistivity along the cubic main axis [100] on a logarithmic and linear scale as function of temperature T. Globally, the behavior is in full accordance with previous observations: FeSi itself exhibits a gapped behavior, implying it to be in an insulating state at $T = 0$ K. To quantify the charge gap, we fit the high-temperature data >200 K (to minimize the influence of the surface states) by $\propto \exp(\Delta_g/2k_BT)$. This approach yields a gap $\Delta_g \sim 700$ K, in good agreement with for instance Ref. [13] (fit not included in the graph).

Alloying with Co induces a MIT, apparent from the drastic change of the overall behavior of ρ from insulating to (badly) metallic, with a residual resistivity of 250 μΩ cm for $x = 0.15$ at lowest temperatures. For $x \geqslant 0.02$, the low-temperature resistivity now has a metallic character $d\rho/dT > 0$, while a broad resistive maximum in an intermediate temperature range ~ 50 K has been associated to a remembrance of the narrow gap band structure of FeSi [31,41] (Fig. 5). Notably, from around 200 K upwards the resistivity for all samples is of similar magnitude, implying that all gap-related features in the resistivity are either overcome by thermal excitations over and/or closing of the gap.

To quantify the MIT we examine the conductivity $\sigma(T) = \rho^{-1}(T)$ plotted for $Fe_{1-x}Co_xSi$ in Fig. 6. From these data we extract the zero-temperature conductivity $\sigma(T \to 0) = \sigma_0$ presented in Fig. 7 as function of alloying x (red left scale). This plot visualizes the fundamental change in behavior from insulating to metallic around $x = 0.01$, in agreement with the Refs. [18,34,38] [σ_0 data from these references included in the plot (orange stars)]. Increasing the Co concentra-

conductivity, with the absolute value of σ_0 increasing by an order of magnitude with varying x from 0.01 to 0.02 (Fig. 6).

It was reported [18] that at temperatures <1 K there is a residual zero-temperature conductivity $\sigma_0 \sim 4$ $(\Omega m)^{-1}$. As we do not cover this temperature range, it might very well also be the case for our crystals. In view of recent studies [17,62] on FeSi and SmB_6 and our own findings, it appears to reflect conducting surface states.

To parametrize the MIT accurately, we draw on the observation of a similarity to classical semiconductors by fitting within critical scaling theory [63–65] our doping dependence of the zero-temperature conductivity with $\sigma_0(x) = \sigma(0)(x - x_{MIT})^\nu$. Certainly, the finite metallic surface conductivity might slightly affect the outcome of our fitting procedure. Still, from a fit to the data we obtain values
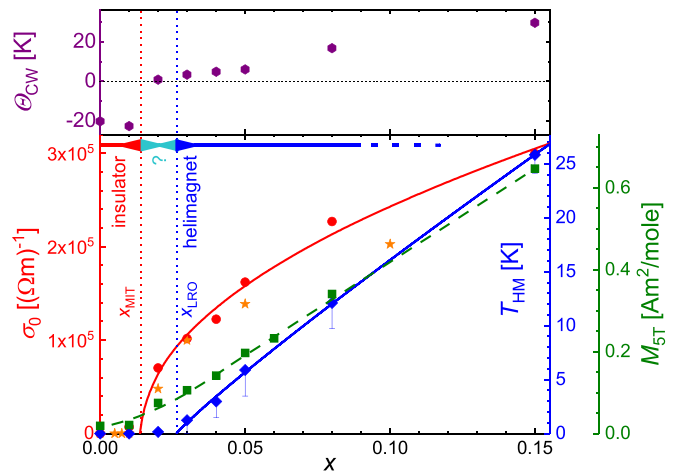

FIG. 7. Composition dependence x of the zero-temperature conductivity σ_0 (left scale, red bullets), magnetic ordering temperature T_{HM} (first right scale, blue diamonds), induced magnetic moment M_{5T} at 5 T (second right scale, green squares), and Curie-Weiss temperature Θ_{CW} (upper panel) of $Fe_{1-x}Co_xSi$, $0 \leqslant x \leqslant 0.15$. In the σ_0 plot we have included the values determined by Chernikov *et al.* [18] and Manyala *et al.* [34,38,65] for their polycrystalline samples (orange stars).
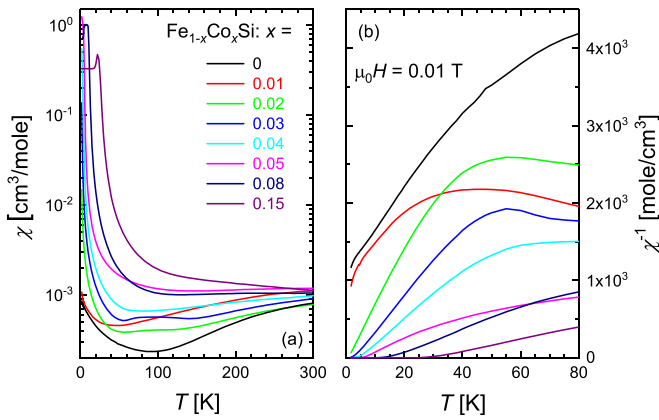
FIG. 8. (a) Temperature-dependent susceptibility $\chi(T)$, plotted on a logarithmic scale, and (b) inverse susceptibility $\chi^{-1}(T)$ of $Fe_{1-x}Co_xSi$, $0 \leqslant x \leqslant 0.15$.

$\sigma(0) = 8.2(1.2) \times 10^5$ $(\Omega m)^{-1}$, $x_{MIT} = 0.014(4)$, and $\nu = 0.50(6)$, consistent with critical scaling theory and similar to previous reports [18,34,38,65] (fit included in the figure as solid red line).

As the next step, knowledge of the underlying magnetic state is necessary. Therefore, in Fig. 8 we plot the susceptibility χ (on a logarithmic scale) and inverse susceptibility χ^{-1} (on a linear scale) of single-crystalline $Fe_{1-x}Co_xSi$ on different temperature scales measured in 0.01 T. For some of the samples ($x = 0.01, 0.02, 0.03$) we observe a weak structure in $\chi(T)$ in an intermediate temperature range $\sim 50 - 150$ K. Zero-field cooled vs field cooled measurement routines reveal a slight history dependence of these signatures, suggesting that they arise from a small amount of ferro-/ferrimagnetic particles in our samples. Using a toy model for a simple estimate, we might assume that these spurious signals arise for instance from single-crystal grain boundaries, which might locally produce small grain boundary Fe inclusions. Then, already less than 0.04% of such grain boundary clusters would be sufficient to account for the history dependence of $\chi(T)$. Therefore, these weak additional magnetic signatures are extrinsic and we will not consider them further.

Starting with FeSi, the well-known paramagnetic susceptibility, with a maximum at higher temperatures ~ 500 K is observed, together with a low-temperature Curie-like upturn, so far attributed to a minute amount of magnetic impurities [13]. Using the argument from Ref. [13], the Curie tail would be accounted for by less than 0.2% per formula unit of $S = \frac{3}{2}$ impurity moments.

The maximum in the susceptibility of FeSi was attributed to an activated behavior across an energy barrier Δ_m in the spin-excitation spectrum [13]. For temperatures $T \ll \Delta_m/k_B$ it allows to fit the susceptibility by $\chi(T) = (C/T) \cdot \exp(-\Delta_m/k_BT)$, with C as a constant that in principle measures the spin of the magnetic moments. Accordingly, we can fit the data for FeSi at temperatures above ~ 150 K with a gap of 515 K, in agreement with Ref. [13] (not shown).

With Co alloying, the high-temperature susceptibility maximum broadens and/or shifts to lower temperatures, and has been replaced by an essentially Curie-Weiss-like susceptibility already at 5% Co doping. If we assume that a shift of the maximum to lower temperatures produces such behavior,

a corresponding gap fit applied to $Fe_{0.99}Co_{0.01}Si$ leads to a substantially reduced gap of ~ 358 K (although the matching with the experiment is substantially worse than for FeSi). It would imply that also with respect to the magnetic properties a minute amount of Co doping is sufficient to suppress gap-like features in the spin-excitation spectra.

At low temperatures all samples exhibit a Curie-Weiss-like upturn of the susceptibility. If we take the approach that this Curie-Weiss-like behavior is associated to magnetic moments with a residual magnetic coupling, then, according to the Curie-Weiss law, the extrapolated intercept of the inverse susceptibility with the temperature axis, the Curie-Weiss temperature Θ_{CW}, is a measure of the coupling strength. Within this concept, we find all samples $Fe_{1-x}Co_xSi$ with $x \geqslant 0.02$ to have a positive Θ_{CW}, corresponding essentially to a finite-ferromagnetic coupling of these samples [see $\chi^{-1}(T)$ in Fig. 8]. As shown in the purple upper panel of Fig. 7, where we display the x dependence of Θ_{CW}, in this compositional range a linear rise of Θ_{CW} with x attests to the strengthening of the magnetic coupling.

Conversely, for FeSi and $Fe_{0.99}Co_{0.01}Si$ the same construction leaves us with antiferromagnetic Curie-Weiss temperatures Θ_{CW} of about -20 K. As pointed out, these samples have spin-excitation gaps much larger than the corresponding values Θ_{CW}, implying that here we consider diluted magnetic moments in an insulator, i.e., a different type of magnetic coupling. Taking these observations together, based on the global behavior of the susceptibility alone, in the metallic regime of the alloying phase diagram we find a finite ferromagnetic coupling, implying that we should observe signatures of long-range magnetic order for these compositions.

To verify this point firmly, we have analyzed the susceptibility and magnetization data for $Fe_{1-x}Co_xSi$ to extract the ordering temperature T_{HM} using various approaches as follows: (a) for our susceptibility data $\chi(T)$ we have determined the second temperature derivative, choosing the inflection point as T_{HM}; (b) we have performed a modified Arrott-plot analysis [66] to derive T_{HM}; (c) we have parametrized the critical behavior close to T_{HM} within the framework of the Heisenberg model [57]; and (d) we have used the Inoue-Shimizu model [67] in the generalization by Brommer [68] as extension of the Landau-description of phase transitions to establish T_{HM}.

We note that using an Arrott-plot or related type of analysis might conceptually be a skewed approach, as the existence of a second-order phase transition at zero magnetic field into a ferromagnetic ground state is assumed. The critical exponents determined this way correspond to a fictious phase transition, which does not take place. Nevertheless, the fictious ferromagnetic transition temperature essentially coincides with the transition into the helimagnetic ground state. Experimentally, it has been demonstrated that with our methods of data treatment it is possible to reproducibly determine the long-range order transition temperatures in this class of compounds [57,58,69]. Therefore, we use these analysis tools to establish a reproducible protocol for the determination of the transition temperatures.

The experimental basis of this analysis are susceptibility data (see above) and magnetization measurements $M(H)$ on our samples $Fe_{1-x}Co_xSi$. As an example, in Fig. 9 we present

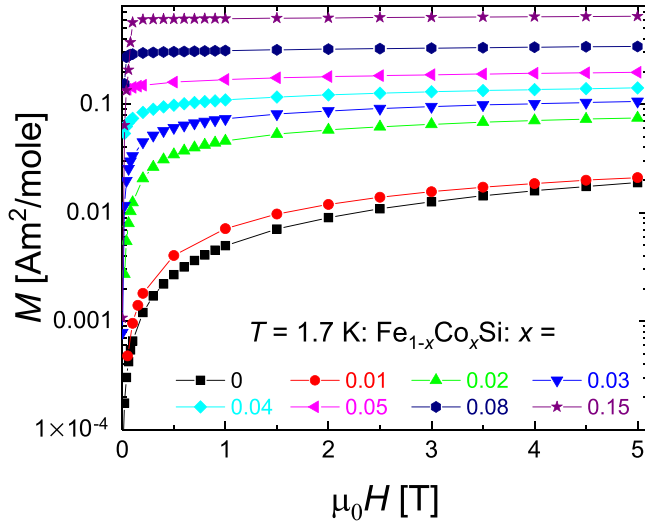FIG. 9. Magnetization M, plotted on a logarithmic scale, as function of field H measured at 1.7 K of $Fe_{1-x}Co_xSi$, $0 \leqslant x \leqslant 0.15$.
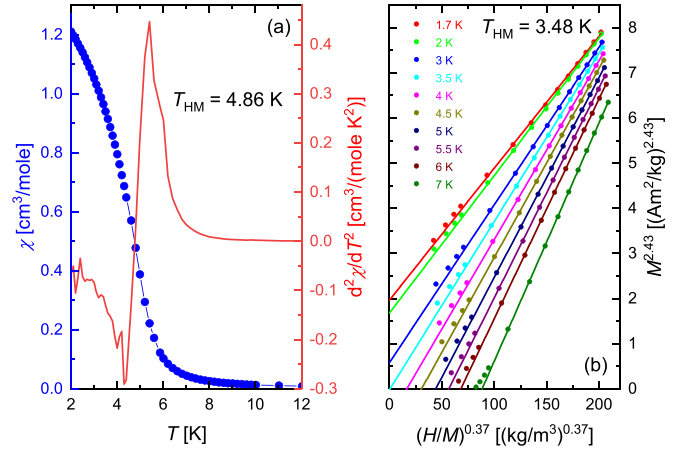

FIG. 10. (a) Temperature-dependent susceptibility $\chi(T)$, measured in $\mu_0 H = 0.01$ T, and second temperature derivative $d^2\chi/dT^2$ of $Fe_{0.95}Co_{0.05}Si$. (b) Modified Arrott-plot analysis of the magnetization of $Fe_{0.95}Co_{0.05}Si$ plotted as $M^{2.43}$ vs $(H/M)^{0.37}$.

$M(H)$ at the base temperature of 1.7 K in fields up to 5 T. Globally, the figure illustrates the expected behavior: for $x \leqslant 0.01$ the magnetization is basically flat and close to zero, but for larger x rises continuously and almost linearly with concentration. Given that the helimagnetic order in $Fe_{1-x}Co_xSi$ is easily field polarized, the basic field dependence of $M(H)$ for $x \geqslant 0.02$ is essentially that of a soft ferromagnet. Notably, only in the insulator-to-metal crossover range $0.01 \rightarrow x \rightarrow 0.03$ there is some curvature in the doping evolution of $M(H)$. This is visualized in Fig. 7, where we include the doping dependence of the induced magnetic moment M_{5T} at 5 T and 1.7 K (green outer right scale).

In the following, we present the different types of analysis and corresponding results for an exemplary case $Fe_{1-x}Co_xSi$, $x = 0.05$, with an extended description of the analysis in the Supplemental Material [70]. Aside from the four approaches we have attempted related types of analysis such as the common Arrott-plot or using different types of criticality (Ising etc.). In result, we find that these approaches either work very badly (Arrott-plot) or do not improve the data parametrization as compared to the approaches discussed here in detail. Overall, the different types of data analysis lead to slightly different ordering temperatures T_{HM}, which we will discuss in more detail below.

We start with the determination of T_{HM} from the inflection point of the susceptibility $\chi(T)$ for $Fe_{0.95}Co_{0.05}Si$ [Fig. 10(a)]. The inverse susceptibility $\chi^{-1}(T)$ in a field of $\mu_0 H = 0.01$ T suggests a magnetic coupling strength somewhat below 10 K (Fig. 8). For low magnetic fields and ignoring demagnetization effects, the inflection point of $\chi(T)$ for a material with a ferri-/ferromagnetic susceptibility signature represents an approximation of the onset of long-range (sublattice) magnetic order. It is derived by numerically calculating the zero intercept of the second derivative $d^2\chi(T)/dT^2$ included in Fig. 10(a). This way, from the figure we obtain a transition temperature $T_{HM}^{susz}(\chi) = 4.86$ K.

Next, as a simple mean-field Arrott-plot analysis does not properly parametrize the experimental data, we have

performed a modified Arrott-plot analysis [66]. In the modified Arrott-plot analysis, by plotting M^y vs $(H/M)^z$, with H the magnetic field strength, the free parameters y and z are varied to maximize the data range of a linear dependence $M^y = A + B \cdot (H/M)^z$, with A, B the derived free fit parameters. In the spirit of the Arrott-plot analysis, the temperature where A becomes zero is then taken as T_{HM}. It is a phenomenological approach to incorporate the scaling laws of critical phenomena in a comparatively simple data handling procedure. In our case, we find as optimum solution a plot $M^{2.43}$ vs $(H/M)^{0.37}$ for our magnetization data on $Fe_{0.95}Co_{0.05}Si$ [Fig. 10(b)]. This in turn leads to an ordering temperature $T_{HM}^{mod} = 3.48$ K.

The concept of scaling laws acting close to a critical temperature T_{HM} is made explicit by observing that $(\frac{H}{M})^{\frac{1}{\gamma}} = a(\frac{T-T_{HM}}{T_{HM}}) + b \cdot M^{\frac{1}{\beta}}$, with critical exponents γ, β. Choosing 3D-Heisenberg criticality, we use $\gamma = 1.386$ and $\beta = 0.365$, resulting in a corresponding plot $M^{\frac{1}{\beta}}$ vs $(\frac{H}{M})^{\frac{1}{\gamma}}$ in Fig. 11(a). From this procedure we obtain $T_{HM}^{Hei} = 5.87$ K.

Finally, for the Landau parametrization of magnetic phase transitions the free energy F of a magnetic material is expanded in multiples of the square of the magnetization M^2. This approach can be refined for mixed compounds etc. by coupling of the different subsystems [67,68]. It results in calculating a Lagrange multiplier λ from the magnetization derivative of the free energy of the system, $dF/dM = \lambda$, with $\lambda = c_1 M + c_3 M^3 + c_5 M^5$ parametrized using the magnetization. As set out in detail in Ref. [68], the minimization procedure yields the parameters $c_1(T)$, $c_3(T)$, and $c_5(T)$, with the minimum of $c_1(T)$ defining T_{HM} and the sign of $c_3(T)$ detailing the character of the phase transition (first or second order). We have carried out this analysis for our samples $Fe_{1-x}Co_xSi$, with the temperature dependence of $c_1(T)$ depicted in Fig. 11(b) for the sample $x = 0.05$. From this Inoue-Shimizu analysis we obtain a transition temperature $T_{HM}^{IS} = 5.89$ K.

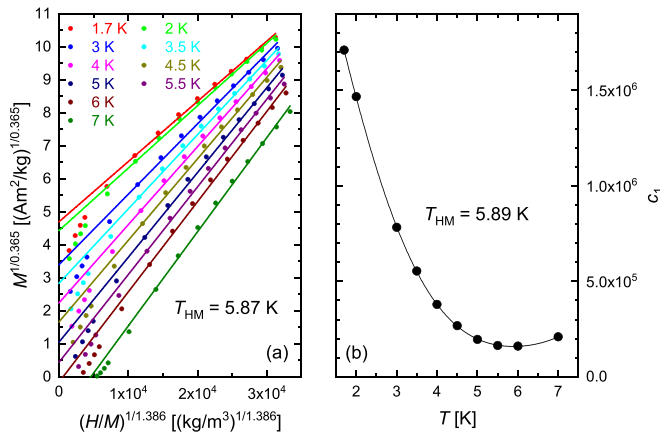FIG. 11. (a) Determination of the transition temperature T_{HM} of $Fe_{0.95}Co_{0.05}Si$ from the magnetization $M(H)$ assuming 3D-Heisenberg criticality. (b) Parameter c_1 as function of temperature from an analysis of $M(H)$ using the Inoue-Shimizu model to extract T_{HM}.

Combining the results from the different types of analysis for our example $Fe_{0.95}Co_{0.05}Si$, we thus obtain a set of transition temperatures T_{HM} in the range 3.48–5.89 K. For further discussion, we decide to take the highest of the four determined values as ordering temperature T_{HM}^*. For graphic representation in Fig. 7 (blue inner right scale) we include the alloying dependence $T_{HM}(x)$ of $Fe_{1-x}Co_xSi$ in the form of $T_{HM}^* - \Delta T_{HM}$, with ΔT_{HM} chosen that all values T_{HM} derived from the different types of analysis are within the error bar (for $x = 0.05$: $\Delta T_{HM} = 2.41$ K). For comparison with the literature data in the Supplemental Material [70] we present a combined plot of the low-doping ($x \leqslant 0.15$) region of the phase diagram including now our experimental results. From the figure it is apparent that the transition temperatures obtained from our study sit right in the middle of the scattered data clouds from literature. For instance, at $x \sim 0.1$ we have determined T_{HM} with an accuracy of about 2 K, where before the reported values varied from 9 to 30 K. This finding validates our approach to firmly establish the phase diagram of $Fe_{1-x}Co_xSi$ by reproducible analysis techniques. Regarding the coefficient $c_3(T)$ specifying if a transition is of first or second order, we find that in the extended Inoue-Shimizu model the value of $c_3(T)$ changes sign within the range of the uncertainty ΔT_{HM} for all samples. We therefore cannot draw a definite conclusion on the nature of the magnetic transition based on the sign of $c_3(T)$.

The dependence $T_{HM}(x)$ now verifies our observation that for samples $Fe_{1-x}Co_xSi$ close to $x = 0.02$ long range magnetic order develops. A fit for instance of the transition temperatures with $T_{HM}^* \propto (x - x_{LRO})^\eta$ yields $x_{LRO} = 0.026(2)$ and $\eta = 0.92(4)$ (solid blue line in Fig. 7). A similar fit, but now taking T_{HM} as average value of the temperature range $T_{HM}^* - \Delta T_{HM}$ yields $x_{LRO} = 0.031(5)$ and $\eta = 0.92(13)$. Altogether, the analysis results in a close-to-linear ($\eta \sim 0.9 - 1$) concentration x dependence of the ordering temperature T_{HM} and a critical concentration x_{LRO} of onset of magnetic order just one percent above the concentration x_{MIT} of the MIT.
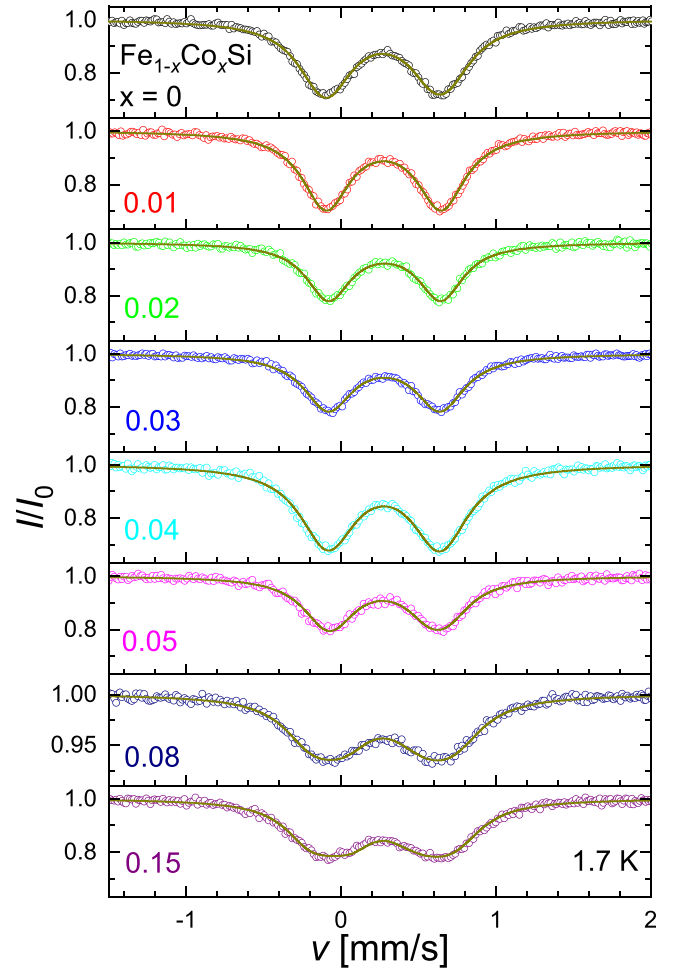

FIG. 12. Overview of the Mössbauer spectra of single-crystalline $Fe_{1-x}Co_xSi$ taken at 1.7 K in zero magnetic field. Solid lines represent fits of the spectra.

Actually, if we consider the error bars of x_{LRO} and x_{MIT}, the two concentrations almost overlap.

To complement our study with a microscopic probe of the magnetic and electronic properties, we have prepared thin slices of single-crystalline samples $Fe_{1-x}Co_xSi$ through polishing with a thickness of a few ten μm to perform Mössbauer spectroscopy. In Fig. 12 we present an overview of the experimental results on these samples at a base temperature of 1.7 K in zero magnetic field. Here we plot the normalized transmission I/I_0, with I_0 being the number of counts at large Doppler velocities far away from the absorption lines. Since it was not possible to define the actual sample thickness in the polishing process to a very accurately defined value, there is a slight thickness variation between different samples by up to ~ 20 μm. This leads to slight variations in the depth of the absorption pattern that can be seen in this plot.

Qualitatively, for all samples a symmetric doublet spectrum with a finite isomer shift is detected. For FeSi, in previous Mössbauer spectroscopy experiments on polycrystalline powder, this absorption spectrum was attributed to a quadrupole splitting from a nonzero electric field gradient, consistent with the Fe site symmetry in the $B20$ structure [3]. Upon alloying with Co, for small concentrations $x \leqslant$
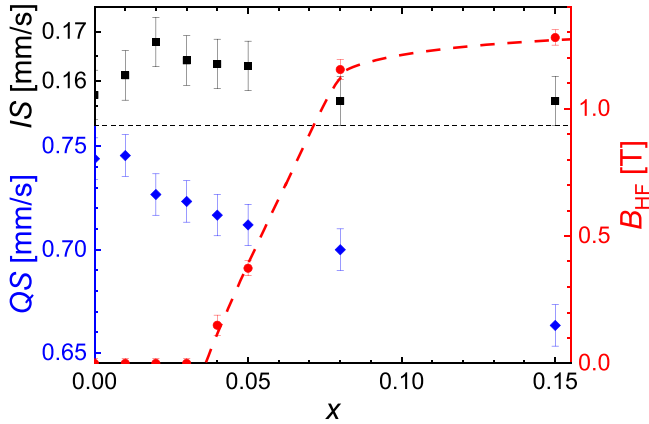
FIG. 13. Compositional dependence x of isomer shift IS, quadrupole splitting QS, and hyperfine magnetic field B_{HF} for single-crystalline $Fe_{1-x}Co_xSi$ at 1.7 K.

FIG. 14. Temperature-dependent Mössbauer spectroscopy data for single-crystalline $Fe_{0.85}Co_{0.15}Si$, demonstrating the broadening of the absorption lines as result of undergoing a long-range magnetic order transition.

0.03 the doublet spectrum persists, while starting with $x = 0.04$ a broadening of the doublet is observed. As has been demonstrated in Ref. [71], this type of line broadening is the indicator of static magnetic order of small magnetic moments; the local magnetic field at the Fe site is still too small for a distinct Fe multiplet to be observable in a Mössbauer experiment. Thus, we conclude that the broadening stems from (helical) magnetic order, consistent with the magnetic phase diagram depicted in Fig. 7, where at an experimental temperature of 1.7 K static local magnetic fields at the Fe site ought to be first observable at $x = 0.04$.

Following the procedure set out in the Refs. [3,20,48] we analyze the data starting with FeSi. In line with these reports, all spectra were fitted with the Mosswinn 4.0i software [72], assuming two Fe sites using the mixed magnetic and quadrupole static Hamiltonian (single crystal) theory, with the same quadrupole splitting QS, isomer shift IS, and the hyperfine magnetic field B_{HF} for both sites and differing only in the angles between QS and B_{HF}, between QS and the gamma ray and B_{HF} and the gamma ray (fits as solid lines in Fig. 12). The values of isomer shifts are given relative to α-Fe at room temperature. Strictly speaking, with our approach we model the helical magnetic state of $Fe_{1-x}Co_xSi$, $x \geqslant 0.04$, as a ferromagnetic one. However, the local magnetic field B_{HF} is very small and thus the local field distribution in such a helical magnet cannot be distinguished in Mössbauer spectroscopy from a weak ferromagnetic one (see discussion of a similar situation in NbFe$_2$ [71,73]).

In our fit of FeSi we use the free parameters IS and QS, with $B_{HF} = 0T$, giving values $IS = 0.157(5)$ mm/s, $QS = 0.744(5)$ mm/s in good agreement with previous reports [3,20,48]. The large experimental line width of 0.42 mm/s is related to the absorber thickness. For the samples $x \geqslant 0.04$ we observe an additional broadening that is attributed to a finite, but small magnetic hyperfine field B_{HF}. From the fit of the experimental data for all samples we obtain the compositional dependence of the fit parameters IS, QS, and B_{HF} summarized in Fig. 13. The general trend of $IS(x)$ and $QS(x)$ is consistent with the findings in previous studies [20,48].

The magnetic hyperfine field exhibits an alloying dependence fully consistent with the magnetic phase diagram
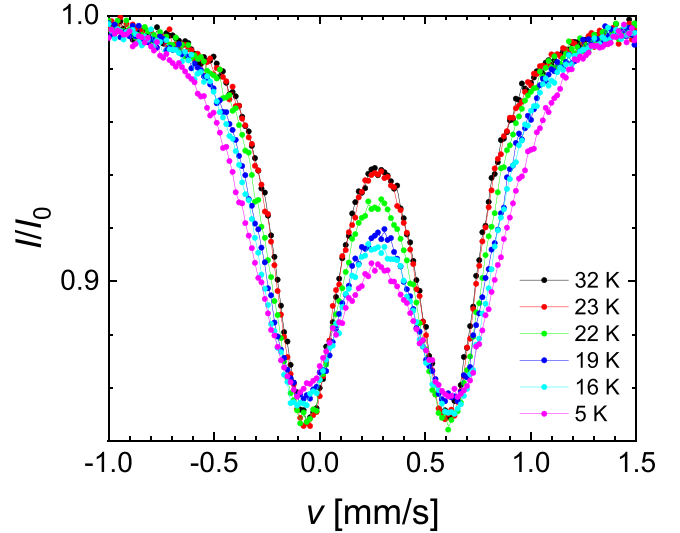
derived from the bulk magnetic properties (Fig. 7). In the temperature range available for the experiment, static magnetic order in the volume of the samples is observable using a microscopic technique for alloying values $x = 0.04$ and above. Consistent with a neutron scattering study on $Fe_{1-x}Co_xSi$ [30], the derived internal magnetic fields in the (sub)-Tesla-range reflect very small ordered magnetic moments $\sim 0.01 - 0.1 \mu_B$/(Fe/Co)-atom and thus weak magnetic order inherent to the vicinity to a magnetic quantum critical point.

Next, we characterize the magnetic order parameter by studying the hyperfine field for selected samples. In Fig. 14 we plot the central ranges of the Mössbauer spectra taken for $Fe_{0.85}Co_{0.15}Si$ as function of temperature. Starting around 23 K, the doublet spectra broaden due to the onset of magnetic order. Following the above fitting routine, from the data we extract the temperature dependence of B_{HF} depicted in Fig. 15. From this plot it is apparent that T_{HM} lies between 23 and 24 K. While again a conceptual argument regarding the applicability of a criticality analysis might be raised, a fit to the data close to the ordering temperature parametrized as $B_{HF} \propto (T_{HM} - T)^\beta$ yields $T_{HM} = 23.03(7)$ K and $\gamma = 0.27(4)$ (solid line in Fig. 15). Most importantly, the value of T_{HM} experimentally obtained from the microscopic probe Mössbauer spectroscopy is in decent agreement with the values derived from the magnetization/susceptibility analysis in the range 24.12–25.83 K, thus validating the analysis of the bulk magnetic data.

IV. DISCUSSION

Summarizing our experimental findings for $Fe_{1-x}Co_xSi$, we have established a close coincidence of the metal-insulator transition at a composition $x_{MIT} = 0.014(4)$ and a quantum critical magnetic-nonmagnetic transition at $x_{LRO} \sim 0.026 - 0.031$. In deriving this finding we have established a protocol that allows to accurately determine magnetic transition
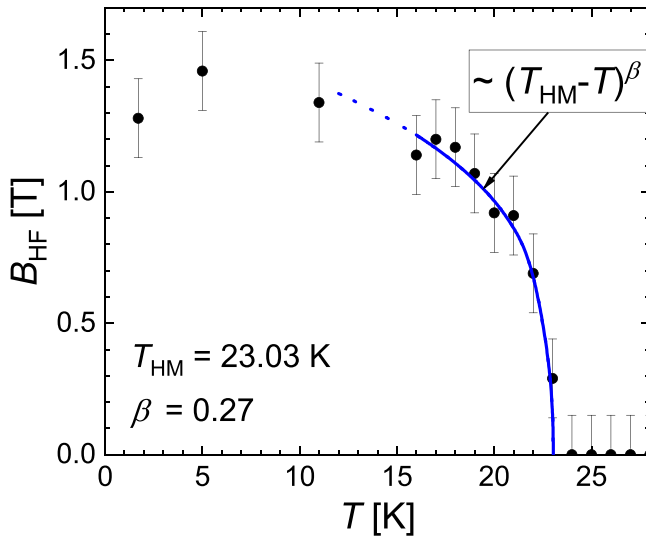
FIG. 15. Temperature dependence of B_{HF} of single-crystalline $Fe_{0.85}Co_{0.15}Si$. The solid line indicates a data parametrization using the fit function indicated close to T_{HM}.

temperatures via both dc magnetic measurements and a local probe technique for this series of compounds. In our data we see no evidence for an extended regime of a coexistence of short- and long-range order as studied for samples of the series with larger x values [56], and thus no evidence for "fuzziness" of the phase transition. In part, it will reflect our choice of experiments, but may also be the result of the alloying range that we have studied in detail. The theoretical arguments at the base of the unusual type of magnetic phase transitions occurring in the $B20$ compounds rely upon a hierarchy of magnetic interactions, i.e., the dominant ferromagnetic exchange, a weaker Dzyaloshinskii-Moriya interaction and a residual magnetic anisotropy energy. Given the large variation of transition temperatures in $Fe_{1-x}Co_xSi$, ranging from (close to) zero at the QPT to about 50 K in the dome of the ordered phase requires a substantial variation of (effective) coupling strengths in this material series. Of course, in this case the detailed character of the magnetic phase transition may vary with x, and may be a very suitable subject of future investigations regarding the character of the phase transition.

With respect to the question if there truly is a difference between x_{MIT} and x_{LRO}, it would represent a very small section $0.014 < x \lesssim 0.031$ of the phase diagram that constitutes a regime of a low-carrier metal with a large magnetic susceptibility and quite unusual physical properties such as the possible formation of magnetic polarons etc. (Fig. 7). However, the question that needs to be addressed first is if x_{MIT} and x_{LRO} can experimentally be firmly distinguished, i.e., the two transitions can be considered to be distinct.

As detailed in Ref. [73] in the analysis of the phase diagram for the quantum critical/weakly ferromagnetic system NbFe$_2$, given that both MIT and LRO in $Fe_{1-x}Co_xSi$ occur in the very dilute Co alloying limit we may assume that a small statistical distribution of local compositions exists in our samples. As set out in Ref. [73] for a basic atomic mixing model, for alloying values of $x = 0.014$ and $x = 0.026 - 0.031$ we may

expect distributions of local compositions of ± 0.002 and 0.003 around the nominal composition.

In an experimental study such as ours this occurrence might slightly affect the actually determined compositional value x of any such transition. For instance, for a magnetic/nonmagnetic transition a distribution of local compositions will tend to promote short range order at the expense of long-range magnetic order. In other words, the experimentally determined value x_{LRO} will be shifted towards the LRO side of the phase diagram, i.e., might be slightly too large in our case. Conversely, for a metal-insulator transition studied by means of conductivity measurements, in samples with a local compositional distribution a percolative metallic conductivity path may form, masking insulating behavior in the bulk of the samples. Therefore, the value x_{MIT} will be shifted towards the insulating side of the MIT, i.e., might be slightly too small in our case.

Hence, for $Fe_{1-x}Co_xSi$ a systematic shift of x_{MIT} to smaller and x_{LRO} to larger compositional values may occur. Then, correcting for this systematic shift and including the experimental error detailed above we would arrive at values $x_{MIT} = 0.016(4)$ and $x_{LRO} \sim 0.023(2) - 0.028(5)$, i.e., matching values within error bars. Therefore, for all practical purposes we have to conclude that MIT and LRO critical compositions are probably experimentally not clearly distinguishable. This observation raises the question about the mechanism(s) behind these (joint) MIT/QPT in $Fe_{1-x}Co_xSi$, which relates back to the issue of the magnetic character of the small gap semiconductor FeSi.

Two main concepts have been put forth to account for the magnetic behavior of FeSi. On the one hand, spin-fluctuation theory has been invoked to account for the basic magnetic properties [74–77]. Taken in combination with band structure calculations [78] it was reported that a single-electron picture captures the essential properties of the small gap semiconductor FeSi. Further, extending the band structure calculations by incorporating a Coulomb interaction U revealed an instability of the band structure towards a metallic magnetic state, with the proposal of a field-induced MIT to occur in FeSi [79,80].

This concept was further worked out [81–83] to account for the properties of the alloying series $FeSi_{1-x}Ge_x$. For this series a first-order insulator-to-ferromagnetic metal transition was reported for $x \approx 0.25$, which was interpreted as result of a tuning of the strength of the Coulomb interaction U with x. It reflects the instability of the band structure of FeSi towards a metallic magnetic state noted in Ref. [79].

On the other hand, the concept of FeSi as a Kondo insulator was proposed, raising the prospect of novel correlation physics apparent in FeSi [12,13,84–86]. Notably, also the first-order insulator-to-ferromagnetic metal transition was presented within this framework [87]. So far, however, direct tests of the Kondo insulator scenario have failed to produce firm evidence for this approach. Only more recently, attempts have been undertaken to merge the different views into a combined picture of correlation effects in a band insulator by using more advanced theoretical tools such as density functional and dynamical mean-field theory [88].

In the context of these previous observations our findings regarding the electronic and magnetic properties of $Fe_{1-x}Co_xSi$ stand out in various aspects. At this point, four

types [89] of "controlled" doping experiments (that is iso-electronic alloying or changing electron count by one) have been performed on FeSi, that is [64,65,81,87,90]: $Fe_{1-x}Co_xSi$, $Fe_{1-x}Mn_xSi$, $FeSi_{1-x}Al_x$, and $FeSi_{1-x}Ge_x$. For these series, both $Fe_{1-x}Mn_xSi$ and $FeSi_{1-x}Al_x$ exhibit MITs for lowering alloying levels, while $FeSi_{1-x}Ge_x$ transforms in a first-order transition into a ferromagnetic metal with alloying.

With respect to the MIT the behavior of $Fe_{1-x}Co_xSi$ is quite similar to $Fe_{1-x}Mn_xSi$ and $FeSi_{1-x}Al_x$. For all systems the critical concentrations x_{MIT} for the MITs is in the low-percentage range. The x dependence of the zero-temperature conductivity σ_0 can be parameterized within critical scaling theory—in other words, the MITs appear to behave in a rather common fashion. In contrast, regarding the transition from a nonmagnetic to a magnetic state, the behavior of $Fe_{1-x}Co_xSi$ is in stark contrast to that of $FeSi_{1-x}Ge_x$. While regarding the alloying dependence the first series exhibits the typical behavior of quantum criticality, for the latter the transition is discontinuous as function of x and of first-order nature. Most remarkably, in $Fe_{1-x}Co_xSi$ the two critical transitions MIT and QPT (almost) coincide regarding their alloying dependence, strongly suggesting a common cause of their appearance.

More specifically, qualitatively, the x dependence of the QPT clearly bears resemblance to related phenomena in weak ferromagnets close to a magnetic instability [91] and which conceptually is in principle accounted for by the self-consistent renormalization theory of spin fluctuations [92]. The experimental data suggest that upon approaching the QPT from the LRO side the ordering temperature T_{HM} and ordered moment μ_{ord} vanish/become very small. The unusual aspect is that quantum criticality must occur in the limit of a very small carrier density as result of the MIT. Such behavior may be qualitatively in line with the modeling put forth in Ref. [88].

This modeling for FeSi implies that spin and charge response are closely linked, this way reproducing the strong temperature dependence of various physical properties and the concomitant crossover from low-temperature insulating to high-temperature metallic behavior. Applying this view to our sample series $Fe_{1-x}Co_xSi$, Co alloying appears to suppress both spin and charge gap in a similar and quite dramatic fashion. This way, with the closing of the spin and charge gaps the ground state of the system transforms via a QPT into a LRO state. Taken together, with the detailed experimental description of the associated properties presented here, we believe that $Fe_{1-x}Co_xSi$ lends itself for a thorough microscopic theoretical study of the underlying physical mechanisms, this in particular in the parameter range of a vanishing carrier density.

[1] W. B. Pearson, *Lattice Spacings and Structures of Metals and Alloys* (Pergamon Press, New York, 1958).

[2] G. Foex, Propriétés magnétiques et ionisation des atomes dans und alliage. Etude expérimentale de quelques siliciures, J. Phys. Radium **9**, 37 (1938).

[3] G. K. Wertheim, V. Jaccarino, J. H. Wernick, J. A. Seitchik, H. J. Williams, and R. C. Sherwood, Unusual electronic properties of FeSi, Phys. Lett. **18**, 89 (1965).

[4] D. Shinoda and S. Asanabe, Magnetic properties of silicides of iron group transition elements, J. Phys. Soc. Jpn. **21**, 555 (1966).

[5] V. Jaccarino, G. K. Wertheim, J. H. Wernick, L. R. Walker, and S. Arajs, Paramagnetic excited state of FeSi, Phys. Rev. **160**, 476 (1967).

[6] C. Pfleiderer, T. Adams, A. Bauer, W. Biberacher, B. Binz, F. Birkelbach, P. Böni, C. Franz, R. Georgii, M. Janoschek *et al.*, Skyrmion lattices in metallic and semiconducting B20 transition metal compounds, J. Phys.: Condens. Matter **22**, 164207 (2010).

[7] I. Dzyaloshinsky, A thermodynamic theory of "weak" ferromagnetism of antiferromagnetics, J. Phys. Chem. Solids **4**, 241 (1958); T. Moriya, Anisotropic superexchange interaction and weak ferromagnetism, Phys. Rev. **120**, 91 (1960).

[8] U. K. Rößler, A. N. Bogdanov, and C. Pfleiderer, Spontaneous skyrmion ground states in magnetic metals, Nature (London) **442**, 797 (2006).

[9] B. Bradlyn, J. Cano, Z. Wang, M. Vergniory, C. Felser, R. Cava, and B. A. Bernevig, Beyond Dirac and Weyl fermions: Unconventional quasiparticles in conventional crystals, Science **353**, aaf5037 (2016).

[10] P. Tang, Q. Zhou, and S.-C. Zhang, Multiple types of topological fermions in transition metal silicides, Phys. Rev. Lett. **119**, 206402 (2017).

[11] H. Wang, S. Xu, X.-Q. Lu, X.-Y. Wang, X.-Y. Zeng, J.-F. Lin, K. Liu, Z.-Y. Lu, and T.-L. Xia, de Haas-van Alphen quantum oscillations and electronic structure in the large-Chern-number topological chiral semimetal CoSi, Phys. Rev. B **102**, 115129 (2020).

[12] G. Aeppli, and Z. Fisk, Kondo insulators, Comments Condens. Matter Phys. **16**, 155 (1992).

[13] Z. Schlesinger, Z. Fisk, H.-T. Zhang, M. B. Maple, J. F. DiTusa, and G. Aeppli, Unconventional charge gap formation in FeSi, Phys. Rev. Lett. **71**, 1748 (1993).

[14] D. Zur, D. Menzel, I. Jursic, J. Schoenes, L. Patthey, M. Neef, K. Doll, and G. Zwicknagl, Absence of Kondo resonance in high-resolution photoemission spectra of monocrystalline $Fe_{1-x}Co_xSi$, Phys. Rev. B **75**, 165103 (2007).

[15] D. Menzel, P. Popovich, N. N. Kovaleva, J. Schoenes, K. Doll, and A. V. Boris, Electron-phonon interaction and spectral weight transfer in $Fe_{1-x}Co_xSi$, Phys. Rev. B **79**, 165111 (2009).

[16] S. Changdar, S. Aswartham, A. Bose, Y. Kushnirenko, G. Shipunov, N. C. Plumb, M. Shi, A. Narayan, B. Büchner, and S. Thirupathaiah, Electronic structure studies of FeSi: A chiral topological system, Phys. Rev. B **101**, 235105 (2020).

[17] Y. Fang, S. Ran, W. Xie, S. Wang, Y. S. Meng, and M. B. Maple, Evidence for a conducting surface ground state in high-quality single crystalline FeSi, Proc. Natl. Acad. Sci. USA **115**, 8558 (2018).

[18] M. A. Chernikov, L. Degiorgi, E. Felder, S. Paschen, A. D. Bianchi, H. R. Ott, J. L. Sarrao, Z. Fisk, and D. Mandrus,

Low-temperature transport, optical, magnetic and thermodynamic properties of $Fe_{1-x}Co_xSi$, Phys. Rev. B **56**, 1366 (1997).

[19] D. Shinoda, Magnetic properties of $Co_{1-x}Fe_xSi$, $Co_{1-x}Mn_xSi$, and $Fe_{1-x}Mn_xSi$ solid solutions, Phys. Status Solidi A **11**, 129 (1972).

[20] I. A. Dubovtsev, F. A. Sidorenko, A. N. Bortnik, T. S. Shubina, and N. P. Filippova, Mössbauer spectra of ^{57}Fe in $Fe_{1-x}Co_xSi$ and $Fe_{1-x}Ni_xSi$, Phys. Status Solidi B **49**, 405 (1972).

[21] P. A. Montano, Z. Shanfield, and P. H. Barrett, Nuclear orientation and Mössbauer studies of alloys of CoSi-FeSi, Phys. Rev. B **11**, 3302 (1975).

[22] D. Bloch, J. Voiron, V. Jaccarino, and J. H. Wernick, $SiFe_{0.5}Co_{0.5}$—A weak itinerant ferromagnet, Phys. Lett. A **51**, 362 (1975).

[23] S. Kawarazaki, H. Yasuoka, Y. Nakamura, and J. H. Wernick, Magnetic properties of $(Fe_{1-x}Co_x)Si$, J. Phys. Soc. Jpn. **41**, 1171 (1976).

[24] J. Beille, D. Bloch, F. Towfio, and J. Voiron, The magnetic properties of Fe_xCo_{1-x} and Fe_xTi_{1-x} alloys, J. Magn. Magn. Mater. **10**, 265 (1979).

[25] J. Beille, J. Voiron, and M. Roth, Long period helimagnetism in the cubic B20 $Fe_xCo_{1-x}Si$ and $Co_xMn_{1-x}Si$ alloys, Solid State Commun. **47**, 399 (1983).

[26] H. Watanabe, Y. Tazuke, and H. Nakajima, Helical spin resonance and magnetization measurement in itinerant helimagnet $Fe_xCo_{1-x}Si$ $(0.3 \leqslant x \leqslant 0.85)$, J. Phys. Soc. Jpn. **54**, 3978 (1985).

[27] M. Motokawa, S. Kawarazaki, H. Nojiri, and T. Inoue, Magnetization measurements of $Fe_{1-x}Co_xSi$, J. Magn. Magn. Mater. **70**, 245 (1987).

[28] A. A. Povzner, S. V. Kortov, and P. V. Geld, Magneto-volume effects in the weak itinerant ferromagnets on the basis of solid solutions of $Fe_{1-y}Mn_ySi$ and $Fe_{1-x}Co_xSi$, Phys. Status Solidi A **114**, 315 (1989).

[29] K. Shimizu, H. Maruyama, H. Yamazaki, and H. Watanabe, Effect of spin fluctuations on magnetic properties and thermal expansion in pseudobinary system $Fe_xCo_{1-x}Si$, J. Phys. Soc. Jpn. **59**, 305 (1990).

[30] K. Ishimoto, M. Ohashi, H. Yamauchi, and Y. Yamaguchi, Itinerant electron ferromagnetism in $Fe_{1-x}Co_xSi$ studied by polarized neutron diffraction, J. Phys. Soc. Jpn. **61**, 2503 (1992).

[31] A. Lacerda, H. Zhang, P. C. Canfield, M. F. Hundley, Z. Fisk, J. D. Thompson, C. L. Seaman, M. B. Maple, and G. Aeppli, Narrow-gap signature of $Fe_xCo_{1-x}Si$, Phys. B: Condens. Matter **186-188**, 1043 (1993).

[32] D. Mandrus, J. L. Sarrao, J. D. Thompson, M. F. Hundley, A. Migliori, and Z. Fisk, Thermal expansion study of $Fe_{1-x}Co_xSi$, Phys. B: Condens. Matter **199-200**, 471 (1994).

[33] G. Aeppli and J. F. DiTusa, Undoped and doped FeSi or how to make a heavy fermion metal with three of the most common elements, Mater. Sci. Eng., B **63**, 119 (1999).

[34] N. Manyala, Y. Sidis, J. F. DiTusa, G. Aeppli, D. P. Young, and Z. Fisk, Magnetoresistance from quantum interference effects in ferromagntes, Nature (London) **404**, 581 (2000).

[35] M. K. Chattopadhyay, S. B. Roy, and S. Chaudhary, Magnetic properties of $Fe_{1-x}Co_xSi$ alloys, Phys. Rev. B **65**, 132409 (2002).

[36] M. K. Chattopadhyay, S. B. Roy, S. Chaudhary, K. J. Singh, and A. K. Nigam, Magnetic response of $Fe_{1-x}Co_xSi$ alloys: A detailed study of magnetization and magnetoresistance, Phys. Rev. B **66**, 174421 (2002).

[37] S. J. Luo, K. L. Yao, and Z. L. Liu, On the magnetic phase transition in $Fe_xMn_{1-x}Si$, J. Magn. Magn. Mater. **265**, 167 (2003).

[38] N. Manyala, Y. Sidis, J. F. DiTusa, G. Aeppli, D. P. Young, and Z. Fisk, Large anomalous Hall effect in a silicon-based magnetic semiconductor, Nat. Mater. **3**, 255 (2004).

[39] D. Menzel, D. Zur, and J. Schoenes, Ultraviolet photoemission spectroscopic and magnetic properties of $Fe_{1-x}Co_xSi$ single crystals, J. Magn. Magn. Mater. **272-276**, 130 (2004).

[40] J. Guevara, V. Vildosola, J. Milano, and A. M. Llois, Half-metallic character and electronic properties of inverse magnetoresistant $Fe_{1-x}Co_xSi$ alloys, Phys. Rev. B **69**, 184422 (2004).

[41] Y. Onose, N. Takeshita, C. Terakura, H. Takagi, and Y. Tokura, Doping dependence of transport properties in $Fe_{1-x}Co_xSi$, Phys. Rev. B **72**, 224431 (2005).

[42] F. P. Mena, J. F. DiTusa, D. van der Marel, G. Aeppli, D. P. Young, C. Presura, A. Damascelli, and J. A. Mydosh, Suppressed reflectivity due to spin-controlled localization in a magnetic semiconductor, Phys. Rev. B **73**, 085205 (2006).

[43] S. V. Grigoriev, S. V. Maleyev, V. A. Dyadkin, D. Menzel, J. Schoenes, and H. Eckerlebe, Principal interactions in the magnetic system $Fe_{1-x}Co_xSi$: Magnetic structure and critical temperature by neutron diffraction and SQUID measurements, Phys. Rev. B **76**, 092407 (2007).

[44] M. Takeda, Y. Endoh, K. Kakurai, Y. Onose, J. Suzuki, and Y. Tokura, Nematic-to-smectic transition of magnetic texture in conical state, J. Phys. Soc. Jpn. **78**, 093704 (2009).

[45] W. Münzer, A. Neubauer, T. Adams, S. Mühlbauer, C. Franz, F. Jonietz, R. Georgii, P. Böni, B. Pedersen, M. Schmidt, A. Rosch, and C. Pfleiderer, Skyrmion lattice in the doped semiconductor $Fe_{1-x}Co_xSi$, Phys. Rev. B **81**, 041203(R) (2010).

[46] V. V. Mazurenko, A. O. Shorikov, A. V. Lukoyanov, K. Kharlov, E. Gorelov, A. I. Lichtenstein, and V. I. Anisimov, Metal-insulator transitions and magnetism in correlated band insulators: FeSi and $Fe_{1-x}Co_xSi$, Phys. Rev. B **81**, 125131 (2010).

[47] X. Z. Yu, Y. Onose, N. Kanazawa, J. H. Park, J. H. Han, Y. Matsui, N. Nagaosa, and Y. Tokura, Real-space observation of a two-dimensional skyrmion crystal, Nature (London) **465**, 901 (2010).

[48] M. K. Forthaus, G. R. Hearne, N. Manyala, O. Heyer, R. A. Brand, D. I. Khomskii, T. Lorenz, and M. M. Abd-Elmeguid, Pressure-induced quantum phase transition in $Fe_{1-x}Co_xSi$ ($x = 0.1, 0.2$), Phys. Rev. B **83**, 085101 (2011).

[49] G. S. Patrin, V. V. Beletskii, D. A. Velikanov, N. V. Volkov, and G. Yu. Yurkin, Effect of cobalt impurity ions on the magnetic and electrical properties of iron monosilicide crystals, J. Exp. Theor. Phys. **112**, 303 (2011).

[50] J. D. Koralek, D. Meier, J. P. Hinton, A. Bauer, S. A. Parameswaran, A. Vishwanath, R. Ramesh, R. W. Schoenlein, C. Pfleiderer, and J. Orenstein, Observation of coherent helimagnons and Gilbert damping in an itinerant magnet, Phys. Rev. Lett. **109**, 247204 (2012).

[51] S. Shanmukharao Samatham, D. Venkateshwarlu, M. Gangrade, and V. Ganesan, Competing localization and quantum interference effects in $Fe_{0.9}Co_{0.1}Si$, Phys. Status Solidi B **249**, 2258 (2012).

[52] P. Milde, D. Köhler, J. Seidel, L. M. Eng, A. Bauer, A. Chacon, J. Kindervater, S. Mühlbauer, C. Pfleiderer, S. Buhrandt, C. Schütte, and A. Rosch, Unwinding of a skyrmion lattice by magnetic monopoles, Science **340**, 1076 (2013).

[53] T. Schwarze, J. Waizner, M. Garst, A. Bauer, I. Stasinopoulos, H. Berger, A. Rosch, C. Pfleiderer, and D. Grundler, Universal helimagnon and skyrmion excitations in metallic, semiconducting and insulating chiral magnets, Nat. Mater. **14**, 478 (2015).

[54] T. Y. Ou-Yang, G. J. Shu, C. D. Hu, and F. C. Chou, Preparation of anomalous magnetoresistance and transport properties of itinerant ferromagnet $Fe_{1-x}Co_xSi$, IEEE Trans. Magn. **51**, 1 (2015).

[55] A. Bauer, M. Garst, and C. Pfleiderer, History dependence of the magnetic properties of single-crystal $Fe_{1-x}Co_xSi$, Phys. Rev. B **93**, 235144 (2016).

[56] L. J. Bannenberg, K. Kakurai, F. Qian, E. Lelièvre-Berna, C. D. Dewhurst, Y. Onose, Y. Endoh, Y. Tokura, and C. Pappas, Extended skyrmion lattice scattering and long-time memory in the chiral magnet $Fe_{1-x}Co_xSi$, Phys. Rev. B **94**, 104406 (2016); L. J. Bannenberg, A. J. E. Lefering, K. Kakurai, Y. Onose, Y. Endoh, Y. Tokura, and C. Pappas, Magnetic relaxation phenomena in the chiral magnet $Fe_{1-x}Co_xSi$: An ac susceptibility study, *ibid.* **94**, 134433 (2016); L. J. Bannenberg, K. Kakurai, P. Falus, E. Lelièvre-Berna, R. Dalgliesh, C. D. Dewhurst, F. Qian, Y. Onose, Y. Endoh, Y. Tokura, and C. Pappas, Universilaty of the helimagnetic transition in cubic chiral magnets: Small angle neutron scattering and neutron spin echo spectroscopy studies of FeCoSi, *ibid.* **95**, 144433 (2017).

[57] L. Zhang, D. Menzel, H. Han, C. Jin, H. Du, J. Fan, M. Ge, L. Ling, C. Zhang, L. Pi, and Y. Zhang, Spin-dimensionality change induced by Co-doping in the chiral magnet $Fe_{1-x}Co_xSi$, Europhys. Lett. **115**, 67006 (2016).

[58] S. Shanmukharao Samatham, K. G. Suresh, and V. Ganesan, Quantum phase transition and non-Fermi liquid behavior in $Fe_{1-x}Co_xSi$ ($x \geqslant 0.7$), J. Phys.: Condens. Matter **30**, 145602 (2018).

[59] S Shanmukharao Samatham, and K. G. Suresh, Critical exponents and universal magnetic behavior of noncentrosymmetric $Fe_{0.6}Co_{0.4}Si$, J. Phys.: Condens. Matter **30**, 215802 (2018).

[60] D. S. Wu, Z. Y. Mi, Y. J. Li, W. Wu, P. L. Li, Y. T. Song, G. T. Liu, G. Li, and J. L. Luo, Single crystal growth and magnetoresistivity of topological semimetal CoSi, Chin. Phys. Lett. **36**, 077102 (2019).

[61] S. Wolgast, C. Kurdak, K. Sun, J. W. Allen, D.-J. Kim, and Z. Fisk, Low-temperature surface conduction in the Kondo insulator SmB_6, Phys. Rev. B **88**, 180405(R) (2013).

[62] J. Jiang, S. Li, T. Zhang, Z. Sun, F. Chen, Z. R. Ye, M. Xu, Q. Q. Ge, S. Y. Tan, X. H. Niu *et al.*, Observation of possible topological in-gap surface states in the Kondo insulator SmB_6 by photoemission, Nat. Commun. **4**, 3010 (2013).

[63] P. A. Lee, and T. V. Ramakrishnan, Disordered electronic systems, Rev. Mod. Phys. **57**, 287 (1985).

[64] J. F. DiTusa, K. Friemelt, E. Bucher, G. Aeppli, and A. P. Ramirez, Metal-insulator transitions in the Kondo insulator FeSi and classic semiconductors are similar, Phys. Rev. Lett. **78**, 2831 (1997).

[65] N. Manyala, J. F. DiTusa, G. Aeppli, and A. P. Ramirez, Doping a semiconductor to create an unconventional metal, Nature (London) **454**, 976 (2008).

[66] A. Arrott and J. E. Noakes, Approximate equation of state for nickel near its critical temperature, Phys. Rev. Lett. **19**, 786 (1967).

[67] J. Inoue and M. Shimizu, Volume dependence of the first-order transition temperature for RCo_2 compounds, J. Phys. F: Met. Phys. **12**, 1811 (1982).

[68] P. E. Brommer, A generalization of the Inoue-Shimizu model, Phys. B: Condens. Matter **154**, 197 (1989).

[69] L. Zhang, D. Menzel, C. Jin, H. Du, M. Ge, C. Zhang, L. Pi, M. Tian, and Y. Zhang, Critical behavior of the single-crystal helimagnet MnSi, Phys. Rev. B **91**, 024403 (2015).

[70] See Supplemental Material at http://link.aps.org/supplemental/10.1103/PhysRevB.109.054414 for details of the data analysis of the susceptibility and magnetization for the whole sample series $Fe_{1-x}Co_xSi$ and comparison of the magnetic phase diagram derived from our data with the literature.

[71] D. Rauch, M. Kraken, F. J. Litterst, S. Süllow, H. Luetkens, M. Brando, T. Förster, J. Sichelschmidt, A. Neubauer, C. Pfleiderer, W. J. Duncan, and F. M. Grosche, Spectroscopic study of metallic magnetism in single-crystalline $Nb_{1-y}Fe_{2+y}$, Phys. Rev. B **91**, 174404 (2015).

[72] Z. Klencsár, Mosswinn 4.0i, revision March 2nd, 2019, http://www.mosswinn.com.

[73] J. Willwater, D. Eppers, T. Kimmel, E. Sadrollahi, F. J. Litterst, F. M. Grosche, C. Baines, and S. Süllow, Muon spin rotation and relaxation study on $Nb_{1-y}Fe_{2+y}$, Phys. Rev. B **106**, 134408 (2022).

[74] Y. Takahashi and T. Moriya, A Theory of nearly ferromagnetic semiconductors, J. Phys. Soc. Jpn. **46**, 1451 (1979).

[75] Y. Takahashi, M. Tano, and T. Moriya, Temperature-induced local moments in FeSi and CoS_2, J. Magn. Magn. Mater. **31-34**, 329 (1983).

[76] Y. Takahashi, Spin-fluctuation theory of FeSi, J. Phys.: Condens. Matter **9**, 2593 (1997).

[77] Y. Takahashi, Theory of magnetization process of FeSi, J. Phys.: Condens. Matter **10**, L671 (1998).

[78] L. F. Mattheiss and D. R. Hamann, Band structure and semiconducting properties of FeSi, Phys. Rev. B **47**, 13114 (1993).

[79] V. I. Anisimov, S. Y. Ezhov, I. S. Elfimov, I. V. Solovyev, and T. M. Rice, Singlet semiconductor to ferromagnetic metal transition in FeSi, Phys. Rev. Lett. **76**, 1735 (1996).

[80] M. Neef, K. Doll, and G. Zwicknagl, Structural, electronic, and magnetic properties of FeSi: Hybrid functionals and non-local exchange, J. Phys.: Condens. Matter **18**, 7437 (2006).

[81] V. I. Anisimov, R. Hlubina, M. A. Korotin, V. V. Mazurenko, T. M. Rice, A. O. Shorikov, and M. Sigrist, First-order transition between a small gap semiconductor and a ferromagnetic metal in the isoelectronic alloy $FeSi_{1-x}Ge_x$, Phys. Rev. Lett. **89**, 257203 (2002).

[82] D. Plencner and R. Hlubina, Magnetically induced metal-insulator transition in $FeSi_{1-x}Ge_x$, Phys. Rev. B **79**, 115106 (2009).

[83] M. Dian and R. Hlubina, Minimal model of the magnetically induced metal-insulator transition: Finite-temperature properties, Phys. Rev. B **89**, 155127 (2014).

[84] Castor Fu, M. P. C. M. Krijn, and S. Doniach, Electronic structure and optical properties of FeSi, a strongly correlated insulator, Phys. Rev. B **49**, 2219(R) (1994).

[85] D. Mandrus, J. L. Sarrao, A. Migliori, J. D. Thompson, and Z. Fisk, Thermodynamics of FeSi, Phys. Rev. B **51**, 4763 (1995).

[86] C. Fu, and S. Doniach, Model for a strongly correlated insulator: FeSi, Phys. Rev. B **51**, 17439 (1995).

[87] S. Yeo, S. Nakatsuji, A. D. Bianchi, P. Schlottmann, Z. Fisk, L. Balicas, P. A. Stampe, and R. J. Kennedy, First-order transition from a Kondo insulator to a ferromagnetic metal in single crystalline $FeSi_{1-x}Ge_x$, Phys. Rev. Lett. **91**, 046401 (2003).

[88] J. M. Tomczak, K. Haule, and G. Kotliar, Signatures of electronic correlations in iron silicide, Proc. Natl. Acad. Sci. USA **109**, 3243 (2012).

[89] We disregard studies on $Fe_{1-x}Ru_xSi$, as spin-orbit coupling might be a relevant factor; see A. Mani, A. Bharathi, S. Mathi Jaya, G. L. N. Reddy, C. S. Sundar, and Y. Hariharan, Evolution of the Kondo insulating gap in $Fe_{1-x}Ru_xSi$, Phys. Rev. B **65**, 245206 (2002).

[90] J. F. DiTusa, K. Friemelt, E. Bucher, G. Aeppli, and A. P. Ramirez, Heavy fermion metal-Kondo insulator transition in $FeSi_{1-x}Al_x$, Phys. Rev. B **58**, 10288 (1998).

[91] M. Brando, D. Belitz, F. M. Grosche, and T. R. Kirkpatrick, Metallic quantum ferromagnets, Rev. Mod. Phys. **88**, 025006 (2016).

[92] T. Moriya, *Spin Fluctuations in Itinerant Electron Magnetism*, Springer Series in Solid-State Sciences Vol. 56 (Springer-Verlag, Berlin, 1985).